Three-dimensionally Ordered Macroporous Mixed Iron Oxide; Preparation and Structural Characterization of Inverse Opals with Skeleton Structure

Masahiro Sadakane,* Chigusa Takahashi, Nobuyasu Kato, Takahito Asanuma, Hitoshi Ogihara, and Wataru Ueda
Catalysis Research Center, Hokkaido University, N-21, W-10, Sapporo 001-0021

(Received February 2, 2006; CL-060149; E-mail: sadakane@cat.hokudai.ac.jp)

Three-dimensionally ordered macroporous (3DOM) materials of polycrystalline spinel- and perovskite-type mixed metal oxide ($ZnFe_2O_4$, $NiFe_2O_4$, and $LaFeO_3$) could be successfully fabricated using colloidal crystal template method in excellent yield. More than 90% of the obtained materials had the 3DOM structure. The crystallites of the spinel- or perovskite-type mixed iron oxide construct struts, tetrahedral and square prism vertexes. The struts connect the tetrahedral and square prism vertexes to produce inverse opals with skeleton structure in three dimensions.

Recently, three-dimensionally ordered macroporous (3DOM) materials with pores sized in the submicrometer range have become the focus of studies because of their application in photonic crystal, catalysis, and separation.[1] To date, most of the 3DOM materials have been synthesized by colloidal crystal template methods as follows: (i) A colloidal crystal template is prepared by ordering monodisperse spheres [e.g., polystyrene (PS) or poly(methyl methacrylate) (PMMA)] into a face-centered cubic close-packed array (opal structure); (ii) interstices in the colloidal crystal are then filled with raw materials, which is solidified to an intermediate composite structure; and (iii) an ordered form (inverse opals) is produced after removing the template by calcination. Three kinds of inverse opal structures have been reported, so-called "residual volume structure," "shell structure," and "skeleton structure."[2]

The skeleton structure consists of strutlike bonds and vertexes, the struts connected vertexes in the former octahedral and tetrahedral voids of the opal structure. These struts and vertexes form a CaF_2 lattice, where 8-coordinated square prism calcium (the former octahedral voids of the opal) vertex is bigger than tetrahedral fluorine (the former tetrahedral voids of the opal) vertex.[3] Models of the skeleton structure were depicted in Figure 1. The views toward (111), (100), and (110) planes of the skeleton structure present hexagonal, square, and lozenge arrangement, respectively, as shown in the Figures 1b–1d.

In this paper, we would like to present the well-ordered inverse opals of polycrystalline mixed iron oxide ($LaFeO_3$, $ZnFe_2O_4$, and $NiFe_2O_4$) with skeleton structure for the first time. This is the first report that both the tetragonal and square prism vertexes are successfully visible. Furthermore, we have achieved to produce the skeleton structure of a variety of mixed metal oxides with controlled metal ratio. To date, only the skeleton structures of monometal oxides and monometals have been seen in the papers,[2,4–7] because it has been difficult to produce mixed metal oxides with controlled metal ratio using common 3DOM preparation methods.[5,8,9]

The PMMA colloidal crystals (diameter: 291 ± 8 nm) was prepared by centrifugation (2500 rpm, 1160 G) of home-made colloidal suspension (ca. 10 g) for 24 h. The obtained template was crushed with an agate mortar and the obtained particles were adjusted into 0.425–2.000 mm using testing sieves (Tokyo Screen, Co., LTD.). The PMMA colloidal crystals were soaked in the ethylene glycol–methanol solution of the metal nitrate mixture (total metal concentration: 2 M) for 4 h. Excess solution was removed from the impregnated PMMA colloidal crystals by vacuum filtration. The obtained sample was allowed to dry in air at room temperature overnight. A 0.5 g amount of the sample was mixed with 2.5 g of quartz sands (10–15 mesh) and calcined in a tubular furnace (i.d. ca. 12 mm) in an air flow (50 $mL \cdot min^{-1}$). The temperature was raised at a rate of 1 $K \cdot min^{-1}$ to 873 K and held for 5 h.

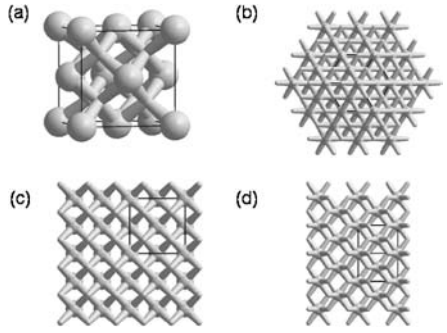

Figure 1. Model of the inverse opals with skeleton structure: (a) cubic unit cell with a lattice constant *a*; (b) view toward (111) plane; (c) view toward (100) plane; (d) view toward (110) plane. In the model, the diameter of the tetrahedral and square prism vertexes was 0.12a and 0.31a, respectively, using Diamond Version 3.1a (copyright Crystal Impact GbR).

The crystal structure (spinel- and perovskite-type) of the obtained samples was confirmed by XRD measurement (Figure S1 in ESI) with reference to JCPDS data bank 22-1012, 10-0325, and 37-1493 for $ZnFe_2O_4$, $NiFe_2O_4$, and $LaFeO_3$, respectively.

Table 1. Physicochemical properties of the samples

Sample	Crystal system Lattice constant/Å[a]	Crystallite size/nm[b]	Pore size /nm[c]
$ZnFe_2O_4$	Cubic $a = 8.447$ (8.441)[d]	23	183 ± 4
$NiFe_2O_4$	Cubic $a = 8.332$ (8.339)[d]	17	169 ± 2
$LaFeO_3$	Orthorombic $a = 5.570$ (5.567)[d] $b = 7.848$ (7.855)[d] $c = 5.552$ (5.553)[d]	25	198 ± 3

[a]Lattice constants were calculated from XRD data using a least-squares method. [b]Crystallite sizes were calculated by Scherrer's equation from XRD data. [c]Pore sizes were estimated from TEM images. [d]Values in parentheses were reported value in the JCPDS data.

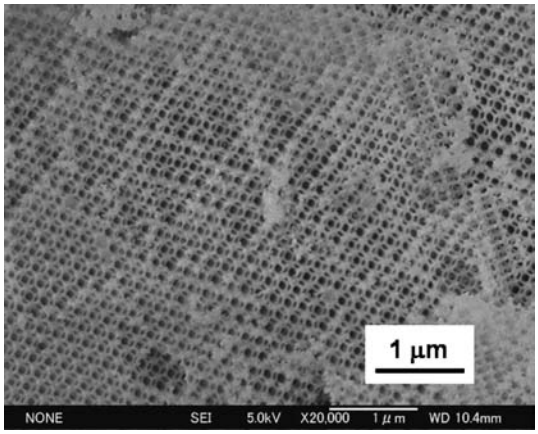

Figure 2. SEM image of the $LaFeO_3$ material of a particle.

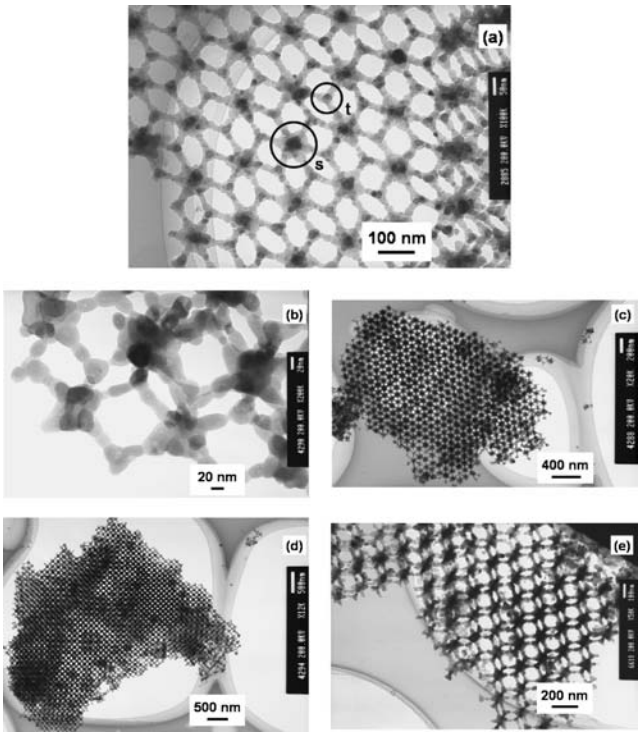

Figure 3. TEM images of the $ZnFe_2O_4$ material. (a) ×100 k, (b) ×200 k (c) ×20 k; view toward (111) plane, (d) ×12 k; view toward (100) plane, and (e) ×50 k; view toward (110) plane of the inversed opal structure. In part (a), a tetrahedral vertex and 8-coordinated square prism vertex were marked as t and s, respectively.

The cell parameters were quite equal to the reported value (Table 1). Furthermore, any by-products could not be detected, indicating that the desired mixed iron oxide was successfully obtained.

The 3DOM structure was first confirmed by SEM. Figure 2 shows SEM image of the $LaFeO_3$ sample as an example. For all the samples, large fractions (more than 90% of particles by SEM image) of the calcined sample were highly ordered porous structure in three dimensions over a range of tens of micrometers (Figure S2 in ESI). Well-ordered air spheres and interconnected struts created a 3DOM material with skeleton structure and the next layer was visible in the SEM image (Figure 2).

The skeleton structure was further characterized by TEM. As seen in Figures 3a and 3b, width of struts (around 20 nm) and grain sizes were similar to the crystallite size calculated by Scherrer's equation from XRD data (Table 1), indicating the grains seen in the Figure 3b are the crystallites. Straight connections of the crystallites construct strutlike bonds, and agglomerations of the crystallites construct vertexes (Figure 3b). The struts connected tetragonal and square prism vertexes (marked as t and s, respectively, in Figure 3a) one after the other to produce inverse opal structure. Continuous ordering of the inverse opal structure was confirmed by observing the hexagonal, square, and lozenge arrangement of the (111), (100), and (110) planes, as shown in the Figures 3b–3e, respectively. In the view toward (100) plane (Figure 3c), long range order (ca. 3 μm long) of the small tetragonal vertexes and big square prism vertexes one after the other in the square arrangement could be observed. Average pore diameters of 183 ± 4 ($ZnFe_2O_4$), 169 ± 2 ($NiFe_2O_4$), and 198 ± 3 ($LaFeO_3$) nm corresponding to a distance between the centers of two neighboring air spheres were estimated by TEM images, and ca. 32–42% of shrinkage from the original PMMA sphere was observed.

In conclusion, the long-range-ordered inverse opals of polycrystalline mixed iron oxides with skeleton structure were successfully produced for the first time. Detailed investigation of formation mechanism of the inversed opals and catalytic application of these materials are now under way.

We would like to thank Mr. K. Sugawara and Mr. Y. Nodasaka for running TEM measurements. M. S. would like to thank Northern Advancement Center for Science and Technology (NOASTEC) and "Hokkaido University Grant Program for supporting young researchers" for financial support.

References and Notes

1 a) R. C. Schroden, A. Stein, in *Colloids and Colloid Assemblies*, ed. by F. Caruso, Wiley-VCH Verlag GmbH & Co. KGaA, Weinheim, **2004**, pp. 465–493. b) A. Stein, R. C. Schroden, *Curr. Opin. Solid State Mater. Sci.* **2001**, *5*, 553. c) A. Stein, *Microporous Mesoporous Mater.* **2001**, *44–45*, 227.
2 a) W. Dong, H. Bongard, B. Tesche, F. Marlow, *Adv. Mater.* **2002**, *14*, 1457. b) W. Dong, H. J. Bongard, F. Marlow, *Chem. Mater.* **2003**, *15*, 568.
3 In the case of two spherical particles A and B, the diameter ratio (dA/dB) which form the octahedron AB6 and tetrahedron AB4 and is about 0.42 and 0.23, respectively.
4 B. T. Holland, C. F. Blanford, T. Do, A. Stein, *Chem. Mater.* **1999**, *11*, 795.
5 H. Yan, C. F. Blanford, J. C. Lytle, C. B. Carter, W. H. Smyrl, A. Stein, *Chem. Mater.* **2001**, *13*, 4314.
6 C. F. Blanford, H. Yan, R. C. Schroden, M. Al-Daous, A. Stein, *Adv. Mater.* **2001**, *13*, 401.
7 S. Sokolov, D. Bell, A. Stein, *J. Am. Ceram. Soc.* **2003**, *86*, 1481.
8 a) S. Sokolov, A. Stein, *Mater. Lett.* **2003**, *57*, 3593. b) H. Yan, C. F. Blanford, W. H. Smyrl, A. Stein, *Chem. Commun.* **2000**, 1477.
9 M. Sadakane, T. Asanuma, J. Kubo, W. Ueda, *Chem. Mater.* **2005**, *17*, 3546.

Published on the web (Advance View) April 1, 2006; DOI: 10.1246/cl.2006.480